NASA Technical Paper 2163

April 1983

X-Ray Photoelectron Spectroscopy and Friction Studies of Nickel-Zinc and Manganese-Zinc Ferrites in Contact With Metals

Kazuhisa Miyoshi and
Donald H. Buckley

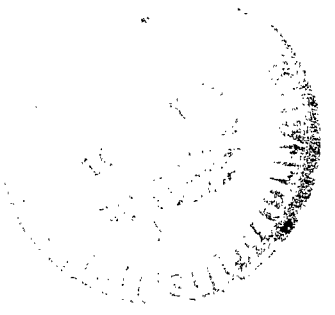

NASA

25th Anniversary
1958-1983

NASA
Technical
Paper
2163

1983

X-Ray Photoelectron Spectroscopy and Friction Studies of Nickel-Zinc and Manganese-Zinc Ferrites in Contact With Metals

Kazuhisa Miyoshi and
Donald H. Buckley
Lewis Research Center
Cleveland, Ohio

NASA
National Aeronautics
and Space Administration

**Scientific and Technical
Information Branch**

Summary

X-ray photoelectron spectroscopy (XPS) analysis and sliding friction experiments were conducted to determine the surface chemistry and friction properties of nickel-zinc (Ni-Zn) and manganese-zinc (Mn-Zn) ferrites. Sliding friction experiments were conducted in ultrahigh vacuum with Ni-Zn and Mn-Zn ferrite flats in contact with various transition metal riders at room temperature. The effect of adsorbed oxygen on friction was also examined.

The results of the investigation indicate that Ni_2O_3 and Fe_3O_4 are present on the Ni-Zn ferrite surface in addition to nominal constituents such as $NiO(NiFe_2O_4)$, ZnO, and Fe_2O_3 and that MnO_2 and Fe_3O_4 are present on the Mn-Zn ferrite surface in addition to nominal constituents such as MnO, ZnO, and Fe_2O_3. The coefficients of friction for Ni-Zn and Mn-Zn ferrites in contact with various transition metals are related to the relative chemical activity of these metals: the more active the metal, the higher is the coefficient of friction. The coefficients of friction for the ferrites correlate with the free energy of formation of the lowest metal oxide. The interfacial bond can be regarded as a chemical bond between the metal atoms and the oxygen anions in the ferrite surfaces. The adsorption of oxygen on cleaned metal and ferrite surfaces increases the coefficients of friction for both the Ni-Zn and Mn-Zn ferrite-metal interfaces.

Introduction

An important subsystem of any computer or communication equipment is its memory or storage function. During the various stages of the computation or communication procedure it is necessary either to store temporarily or permanently computer results for use in later calculations or to store communication information that must be referred to over a long period of time. Among the many physical possibilities that are available to perform these storage functions are magnetic tape, magnetic disk, magnetic drum, photographic film, recirculating delay lines, and thin magnetic films.

Magnetic recording has been developed to a highly refined system. The term "magnetic recording" can be applied to any recording technique in which some phase of magnetics is intimately associated with either the recording or playback process.

Both Ni-Zn and Mn-Zn ferrites are ceramic semiconductors and are becoming increasingly important as magnetic materials used for highly developed magnetic recording devices. The Ni-Zn ferrites have been used for computer memory systems, such as magnetic recording disk files; the Mn-Zn ferrites have been used for video and audio tape recorders in order to enhance certain desirable properties and to suppress undesirable ones in certain applications. In most devices of magnetic recording and playback, recording is conducted with a magnetic head (slider) in sliding or intermittent contact with a magnetic medium, such as a magnetic tape or disk. A small amount of wear of the magnetic head and medium may render the recording process unreliable. The magnetic head and medium therefore must have good wear resistance and low friction.

The tribological properties of ferrites have been extensively studied, and considerable information is available (refs. 1 to 21). It must be stressed, however, that many of the observed fundamental properties and effects are not completely understood.

Miyoshi and Buckley commenced fundamental studies on the friction and wear behavior of single-crystal Mn-Zn ferrite in order to gain an understanding of the tribological properties of ferrites (refs. 22 to 24). The results indicated that the coefficients of friction for the ferrite in contact with various metals are related to the relative chemical activity of the metals: the more active the metal, the higher the coefficient of friction. The present study extends that work to the tribological properties of hot-pressed Ni-Zn and Mn-Zn ferrites in the polycrystalline form.

This report discusses the surface chemistry and friction properties of hot-pressed, polycrystalline Ni-Zn and Mn-Zn ferrites in contact with various transition metals. The effect of adsorbed oxygen on friction is also examined. The surface chemistry of the ferrites was analyzed by X-ray photoelectron spectroscopy (XPS). Sliding friction experiments were conducted with both a Ni-Zn and a Mn-Zn ferrite specimen in contact with polycrystalline metal pins at room temperature. All friction experiments were conducted with loads of 0.05 to 0.2 N, at a sliding velocity of 5×10^{-2} mm/sec, and in a vacuum of 30 nPa.

Materials

The hot-pressed polycrystalline Ni-Zn ferrite (66.6-wt % Fe_2O_3, 11.1 wt % NiO, and 22.2 wt % ZnO) and Mn-Zn ferrite (69.1-wt % Fe_2O_3, 15.2-wt % MnO, and 15.7-wt % ZnO) are ceramic semiconductors. Compositions are as certified by the manufacturer.

All the metals were polycrystalline. The titanium was 99.97 percent pure, and all the other metals (Co, Cr, Fe, Ni, Re, Rh, V, W, and Zr) were 99.99 percent pure.

Apparatus and Procedure

Apparatus

An apparatus capable of measuring adhesion, load, and friction was mounted in an ultra-high-vacuum

system (fig. 1). The vacuum system contained X-ray photoelectron spectroscopy. The major components shown in figure 1 include the electron energy analyzer, the X-ray source, and the ion gun used for ion sputter etching. The X-ray source contains a magnesium anode.

Specimen Preparation

The sliding surfaces of Ni-Zn and Mn-Zn ferrite flats were polished first with diamond powder approximately 3 μm in diameter and then with Al_2O_3 powder 1 μm in diameter. The polished surfaces were smooth, bright, and lustrous without pitting.

The sliding surfaces of the polycrystalline metal riders (pins) were hemispherical and were polished first with diamond powder 3 μm in diameter and then with Al_2O_3 powder 1 μm in diameter. The radius of curvature of the metal riders was 0.79 mm.

Procedure

The surfaces of the flat and rider specimens were rinsed with absolute ethanol before the experiments. For the experiments in vacuum the specimens were placed in the vacuum chamber, and the system was evacuated and baked out to achieve a pressure of 30 nPa (10^{-10} torr). The flat and rider specimens were ion sputter cleaned. Ion sputter etching was performed with a beam energy of 3000 electron volts (eV) at 20-mA beam current with an argon pressure of 7×10^{-4} Pa. The ion beam was continuously rastered over the specimen surface. After sputter etching the system was reevacuated to a pressure of 30 nPa or lower. The surface cleanliness was verified by XPS analysis.

In situ friction experiments were conducted with the sputter-cleaned ferrite flat and metal rider specimens. A load of 0.05 to 0.2 N was applied to the rider-flat contact by deflecting the beam, as shown in figure 1. To obtain consistent experimental conditions, the time in contact before sliding was 30 sec. Both load and friction forces were continuously monitored during a friction experiment. Sliding velocity was 5×10^{-2} mm/sec, with a total sliding distance of 2 to 3 mm. The coefficients of friction reported herein were obtained by averaging three to five measurements. The standard deviations of the measured values are within 4 percent of the mean value.

In those experiments designed to examine the effect of adsorbed oxygen on friction, atomically sputter-cleaned ferrite and metal surfaces were exposed to 1000 L ($L = 1 \times 10^{-6}$ torr sec) of O_2 with an oxygen pressure of 1×10^{-6} torr. At completion of the exposure the vacuum system was reevacuated to a pressure of 30 nPa or lower. The surface chemistry of the specimens was examined by XPS analysis. Friction experiments were conducted with the ferrite and metal specimens that were exposed to oxygen in the same manner as with atomically clean specimens.

The instrument was calibrated regularly. The analyzer calibration was determined by assuming the binding energy for the gold 4f 7/2 peak to be 83.8 eV. All survey spectra, scans of 1000 or 1100 eV, were taken at a pass energy of 50 eV, which provided an instrumentation resolution of 1 eV at room temperature. The MgKα X-ray was used with an X-ray source power of 400 W (10 kV − 40 mA). The narrow scans of individual peaks are just wide enough to encompass the peaks of interest and were obtained with a pass energy of 25 eV at room temperature.

To determine accurately the energy and the shape of the peaks, spectra were recorded several times. The energy resolution was 2 percent of the pass energy, that is, 0.5 eV. The peak maxima could be located to ± 0.1 eV. The reproducibility of peak height was good, and the probable error in the peak heights ranged from ± 2 to ± 8 percent. The peak ratios were generally good to ± 10 percent or less.

Results and Discussion

Microstructure

To establish the exact crystalline state of the Ni-Zn ferrite, grain boundary structures were examined by scanning electron microscopy, transmission electron microscopy, and diffraction. The transmission electron microscope was operated at 100 kV.

A typical example of the structure of the Ni-Zn ferrite surface as chemically etched with an HCl solution at 50° C is shown in figure 2. The etched surface contained grain boundaries, pits, and scratches. Grain size was obtained by averaging the measurements of 50 grains or more in scanning electron micrographs. The grain size of the Ni-Zn ferrite was about 8 μm.The grain size of Mn-Zn ferrite was about 24 μm.

Typical examples of the grain boundary microstructure of the Ni-Zn ferrite examined by transmission electron microscopy and diffraction are shown in figures 3 to 5. (The Ni-Zn ferrite specimens were thinned by ion etching.) Clear grain boundaries were observed, as shown in figures 3 to 5. Grain boundaries that were nearly perpendicular to the ferrite surface contained single lines (fig. 3). Grain boundaries that were not perpendicular to the ferrite surface contained parallel fringes (figs. 4 and 5).

Single-crystal patterns taken from a grain included diffraction spots and Kikuchi lines, as indicated in figures 3 to 5.

The ion-etched Ni-Zn ferrite specimens have different etch patterns reflecting different crystallographic orientations of the grains. The etch patterns are related to the anisotropic etching rate of the grain surface.

Energy-dispersive X-ray analysis was conducted on the Ni-Zn ferrite. Figure 6 presents a typical energy-dispersive X-ray profile of this ferrite. The profile clearly indicates iron, nickel, and zinc.

XPS Analysis

Ni-Zn ferrite. – The XPS survey spectra of the Ni-Zn ferrite surfaces obtained before sputter cleaning reveal primarily oxygen and carbon contamination peaks. An XPS spectrum of the ferrite surface after sputter cleaning for 20 min is shown in figure 7. The carbon contamination peak has nearly disappeared from the spectrum. In addition to oxygen and iron, the XPS peaks indicate nickel and zinc on the surface.

The XPS spectra of Ni_{2p}, Zn_{2p}, Fe_{2p}, and O_{1s} obtained from narrow scans on the Ni-Zn ferrite surface are presented in figure 8. The $Ni_{2p3/2}$ photoelectron emission lines of the Ni-Zn ferrite after argon sputter cleaning are split asymmetrically into two peaks at 853.3 and 855.0 eV (fig. 8(a)). The binding energies of the two peaks match those of both $NiFe_2O_4$ (or Ni^{2+} ion in NiO) and Ni_2O_3, respectively (refs. 25 and 26). The $Zn_{2p3/2}$ photoelectron lines for the Ni-Zn ferrite peak at 1021.7 eV (fig. 8(b)), which is associated with ZnO. The $Fe_{2p3/2}$ photoelectron lines peak at 710.8 eV (fig. 8(c)). The binding energy matches that for both Fe_2O_3 and $NiFe_2O_4$, which are extremely close in energy and difficult to distinguish in the data of figure 8(c). In figure 8(d), in addition to the adsorbed oxygen contamination peaks, the O_{1s} peak associated with Fe_2O_3 is observed on the as-received Ni-Zn ferrite surface. The peak intensity at 530 eV associated with Fe_2O_3 increased with an increase in sputtering time up to 20 min.

Table I summarizes the various constituents present on the Ni-Zn ferrite surface and their relative concentrations before and after sputtering. The relative concentrations of adventitious hydrocarbon, which was present on the as-received Ni-Zn ferrite and was introduced during the specimen preparation process, was about 79 at. % (table I(a)). After sputtering no carbon was evident on the Ni-Zn ferrite surface. The concentrations of nickel oxides (NiO and Ni_2O_3), ZnO, and Fe_2O_3 on the Ni-Zn ferrite surface as obtained from the XPS spectra are interesting in that on the surface after sputtering the concentration of ZnO is less than that of nickel oxides, while in the bulk the concentration of ZnO is greater than that of nickel oxides (table I). The results suggest that zinc may segregate and be sputtered away from the surface during argon ion sputtering.

Mn-Zn ferrite. – The XPS survey spectra of the Mn-Zn ferrite surface obtained before sputter cleaning reveal primarily oxygen and carbon contamination peaks, as shown in figure 9. An XPS spectrum of the ferrite surface after sputter cleaning for 20 min is shown in figure 9. The carbon contamination peak has nearly disappeared from the spectrum after sputter cleaning. In addition to oxygen and iron, the XPS peaks clearly indicate manganese and zinc on the surface.

TABLE I. – VARIOUS CONSTITUENTS ON Ni-Zn FERRITE SURFACE AND THEIR CONCENTRATIONS

(a) Elements

Surface treatment in vacuum chamber	Concentration, at. %				
	Ni	Zn	Fe	O	C
No treatment	1	1	3	16	79
Sputtering	9	5	30	56	0

(b) Oxides

	Surface treatment in vacuum chamber	Concentration, mol %		
		Nio (and Ni_2O_3)	ZnO	Fe_2O_3 (Fe_3O_4)
Surface	No treatment	17	17	66
	Sputtering	20	10	70
Bulk		11.5	20.0	68.4

Figure 10 presents the XPS spectra of Mn_{2p}, Zn_{2p}, Fe_{2p}, and O_{1s} obtained from narrow scans on the Mn-Zn ferrite surfaces.

The $Mn_{2p3/2}$ photoelectron emission lines of the Mn-Zn ferrite after cleaning include two peaks (fig. 10(a)). The binding energies of the peaks match both MnO and the Mn^{+2} ion in the oxide (MnO_2)(ref. 25). The Zn_{2p} photoelectron lines for the Mn-Zn ferrite peak at 1021.7 eV (fig. 10(b)), which is associated with ZnO. The $Fe_{2p3/2}$ photoelectron lines include Fe_2O_3 as well as a small amount of Fe_3O_4 (fig. 10(c)). The O_{1s} peaks obtained from the as-received surface (fig. 10(d)) are associated with adsorbed oxygen contamination and Fe_2O_3. After sputtering, the XPS peaks indicate Fe_2O_3 on the Mn-Zn ferrite surface.

Table II summarizes various constituents present on the Mn-Zn ferrite surface and their relative concentrations before and after sputtering. The relative concentration of hydrocarbon contaminant is 70 at. %. After sputtering no carbon is evident on the Mn-Zn ferrite surface. As with the Ni-Zn ferrite, on the surface the concentration of ZnO is less than that of manganese oxides, while in the bulk the concentration of ZnO is greater than that of manganese oxides. This result is consistent with Mn-Zn ferrite chemistry.

TABLE II. – VARIOUS CONSTITUENTS ON Mn-Zn FERRITE SURFACE AND THEIR CONCENTRATIONS

(a) Elements

Surface treatment in vacuum chamber	Concentration, at. %				
	Mn	Zn	Fe	O	C
No treatment	3	1	4	21	71
Sputtering	11	3	29	57	0

(b) Oxides

	Surface treatment in vacuum chamber	Concentration, mol %		
		Mn (and MnO_2)	ZnO	Fe_2O_3 (Fe_3O_4)
Surface	No treatment	36	15	49
	Sputtering	26	7	67
Bulk		15.7	14.1	70.2

Friction

Effect of Metal Activity on Friction

The relative chemical activity of the transition metals (metals with partially filled d-shells) as a group can be ascertained from their percentage d-bond character as shown by Pauling (ref. 27). The frictional properties of metal-metal and metal-ceramic contacts have been shown to be related to this character (refs. 28 to 32). The greater the percentage of d-bond character, the less active is the metal and the lower is the coefficient of friction.

Sliding friction experiments were conducted with ferrite flats in contact with a number of transition metal riders. The friction traces with metal-ferrite couples are generally characterized by smoothly fluctuating behavior with no evidence of stick-slip, but the traces with a very chemically active metal such as titanium are characterized by stick-slip fluctuating behavior (fig. 11). The coefficients of friction for various metals sliding on ferrite were unaffected by load in the range 0.05 to 0.2 N.

The coefficients of friction for various metals in sliding contact with Ni-Zn and Mn-Zn ferrites are presented in figure 12 as a function of the d-bond character of the transition metal. There appears to be good correlation between the coefficient of friction and the chemical activity of the transition metal. Titanium, a chemically active metal, exhibits a considerably higher coefficient of friction in contact with ferrite than does rhodium, a less active metal. This result is consistent with the authors' earlier studies conducted with single crystals of SiC, diamond, and Mn-Zn ferrite (refs. 29, 31, and 32.).

The coefficients of friction with single-crystal Mn-Zn ferrite {110} plane (fig. 12(b)) are lower than those of the hot-pressed, polycrystalline Mn-Zn ferrite. This difference in friction may be in accord with effects of crystallographic orientation and grain boundary as well as impurities contained in the crystals. The crystallographic plane and direction can play a significant role in the friction behavior of ferrite (refs. 22 and 24). Sliding along the direction that is most closely packed minimizes adhesion and friction. Note that {110} ⟨110⟩ is the slip system of Mn-Zn ferrite.

The coefficients of friction can also be correlated with the free energy of formation of the lowest metal oxides, as shown in figure 13. This correlation is consistent with the results of Pepper (ref. 32), that is, the shear coefficients of the clean metal (Ag, Cu, Ni, and Fe)–sapphire contacts correlate with the free energy of formation of the lowest metal oxides. The correlation shown in figure 13 is consistent with the concept that the metal-ferrite bond at the interface is primarily a chemical bond between the metal atoms and the large oxygen anions in the ferrite surface and that the strength of this bond is related to the oxygen-metal bond strength in the metal oxide (refs. 32 to 36).

All the metals shown in figure 12 transferred to the surfaces of the ferrites. In general the less active the metal, the less transfer to the ferrite. Titanium, having a much stronger chemical affinity to the elements of the ferrite, exhibited the greatest amount of transfer (refs. 22, 23, and 31).

Effect of Oxygen Adsorption on Friction

Figure 14 shows the coefficients of friction for various metals in contact with the ferrites as a function of the d-bond character of the metal, Both metal and ferrite specimens were exposed to O_2 gas. The data indicate a decrease in friction with an increase in d-bond character. The adsorption of oxygen on argon-sputter-cleaned metal and ferrite surfaces produces two effects: (1) the metal oxidizes and forms a oxide surface layer; and (2) the layer increases the coefficients of friction for both Ni-Zn and Mn-Zn ferrite-to-metal interfaces.

The present results are consistent with those shown in reference 32. It is suggested in reference 32 that oxygen exposures do strengthen metal-sapphire contact and increase friction.

The enhanced bond of the metal oxide to sapphire was due to the formation of a complex oxide when metal contact was established. The enhanced coefficient of friction indicated in figure 14 may be due to the foregoing mechanism of bonding.

Conclusions

As a result of the XPS analysis and the sliding friction experiments conducted with hot-pressed, polycrystalline nickel-zinc and manganese-zinc ferrite surfaces in sliding contact with various transition metals, the following conclusions were drawn.

1. Ni_2O_3 and Fe_3O_4 are present on the Ni-Zn ferrite surface in addition to nominal constituents such as NiO ($NiFe_2O_4$), ZnO, and Fe_2O_3. MnO_2 and Fe_3O_4 are present on the Mn-Zn ferrite surface in addition to nominal constituents such as MnO, ZnO, and Fe_2O_3.

2. The coefficients of friction for Ni-Zn and Mn-Zn ferrites in contact with various metals are related to the relative chemical activity of these metals: the more active the metal, the higher is the coefficient of friction. The coefficients of friction for the ferrites correlate with the free energy of formation of the lowest metal oxide. The interfacial bond can be regarded as a chemical bond between the metal atoms and the oxygen anions in the ferrite surfaces. The adsorption of oxygen on the clean metal and ferrite surfaces increases the coefficients of friction as a result of the oxide surface layer on both the Ni-Zn and Mn-Zn ferrite-to-metal interfaces.

Lewis Research Center
National Aeronautics and Space Administration
Cleveland, Ohio, December 7, 1982

References

1. Tanaka, K.; et al.: Friction and Wear in the Sliding of VTR Head Against Magnetic Tape. I—Contact Force and Frictional Force. J. Jpn. Soc. Precis. Eng., vol. 40, no. 7, 1974, pp. 550–556.
2. Tanaka, K.; et al.: Friction and Wear in the Sliding of VTR Head Against Magnetic Tape. II—Wear of VTR Head Made of a Ferrite Single Crystal. J. Jpn. Soc. Precis. Eng., vol. 40, no. 8, 1974, pp. 651–657.
3. Tanaka, K.; Miyoshi, K.; and Murayama, T.: Friction and Wear in the Sliding of VTR Head Against Magnetic Tape. III—Effect of Wear on the Output Signal Level. J. Jpn. Soc. Precis. Eng., vol. 40, no. 9, 1974, pp. 785–792.
4. Tanaka, K.; and Miyoshi, K.: Friction and Wear on Magnetic Tape. I—Frictional Behavior. J. Jpn. Soc. Lubr. Eng., vol. 19, no. 9, 1974, pp. 645–653.
5. Tanaka, K.; et al.: Friction and Deformation of Mn-Zn Ferrite Single Crystals. I—Contact and Friction of Ferrite Single Crystals. J. Jpn. Soc. Precis. Eng., vol. 41, no. 2, 1975, pp. 148–154.
6. Tanaka, K.; et al.: Friction and Deformation of Mn-Zn Ferrite Single Crystals—Frictional Properties and Deformation. Bull. Jpn. Soc. Precis. Eng., vol. 9, no. 1, 1975, pp. 27–34.
7. Tanaka, K.; et al.: Friction and Deformation of Mn-Zn Ferrite Single Crystals—Crack Formation. Bull. Jpn. Soc. Precis. Eng., vol. 9, no. 2, 1975, pp. 47–48.
8. Tanaka, K.; et al.: Abrasive Wear of Mn-Zn Ferrite. I—Effects of Abrasive Grain Size and Contact Pressure. J. Jpn. Soc. Precis. Eng., vol. 41, no. 9, 1975, pp. 896–902.
9. Tanaka, K.; et al.: Friction and Deformation of Mn-Zn Ferrite Single Crystals. Proceeding of JSLE-ASLE International Lubrication Conference, T. Sakurai, ed., Elsevier Scientific Publishing Co., 1976, pp. 58–66.
10. Miyoshi, K.; Tanaka, K.; and Murayama, T.: Friction and Wear of Magnetic Tape. II—Effects of Surface Roughness of Countersurface on Friction. J. Jpn. Soc. Lubr. Eng., vol. 21, no. 11, 1976, pp. 756–763.
11. Miyoshi, K.; Tanaka, K.; and Murayama, T.: Abrasive Wear of Mn-Zn Ferrite. II—Effects of Sliding Speed and Abrasive/Carrier Fluid Ratio. J. Jpn. Soc. Precis. Eng., vol. 43, no. 4, 1977, pp. 483–488.
12. Miyoshi, K.; Tanaka, K.; and Murayama, T.: Abrasive Wear of Mn-Zn Ferrite. III—Deformed Crystalline Layers and Surface Cracking. J. Jpn. Soc. Precis. Eng., vol. 43, no. 10, 1977, pp. 1192–1197.
13. Miyoshi, K.; et al.: Tape Lapping of Manganese-Zinc Ferrite Crystals. I—Frictional Properties and Abrasiveness of Lapping Tapes. J. Jpn. Soc. Precis. Eng., vol. 43, no. 12, 1977, pp. 1395–1401.
14. Carroll, J. F., Jr.; and Gotham, R. C.: The Measurement of Abrasiveness of Magnetic Tape. IEEE Trans. Magn., vol. mag-2, no. 1, Mar. 1966, pp. 6–13.
15. Talke, F. E.; and Su, J. L.: The Mechanism of Wear in Magnetic Recording Disk Files. Tribol. Int., vol. 8, no. 1, Feb. 1975, pp. 15–20.
16. Kehr, W. D.; Meldrum, C. B.; and Thornley, R. F. M.: The Influence of Grain Size on the Wear of Nickel-Zinc Ferrite by Flexible Media. Wear, vol. 31, 1975, pp. 109–117.
17. Tanaka, K.; and Miyazaki, O.: Wear of Magnetic Materials and Audio Heads Sliding Against Magnetic Tape. Wear, vol. 66, 1981, pp. 289–306.
18. Hahn, F. W., Jr.: Materials Selection for Digital Recording Heads. Proceedings of Wear Materials. Wear 1977, W. A. Glaeser, K. C. Ludema, and S. K. Rhee, eds., ASME, 1977, pp. 199–203.
19. Begelinger, A.; and deGee, A. W. J.: Wear Measurements Using Knoop Diamond Indentations. Wear, vol. 43, 1979, pp. 259–261.
20. Van Groenou, A. Broese; Maan, N.; and Veldkamp, J. D. B.: Scratching Experiments on Various Ceramic Materials. Philips Res. Rep., vol. 30, no. 5, 1975, pp. 320–359.
21. Miyoshi, K.: Lapping of Manganese-Zinc Ferrite by Abrasive Tape. Lubr. Eng., vol. 38, no. 3, Mar. 1982, pp. 165–172.
22. Miyoshi, K.; and Buckley, D. H.: Friction and Wear of Single-Crystal Manganese-Zinc Ferrite. Wear, vol. 66, 1981, pp. 157–173.
23. Miyoshi, K.; and Buckley, D. H.: Friction and Wear of Single-Crystal and Polycrystalline Manganese-Zinc Ferrite in Contact with Various Metals. NASA TP-1059, 1977.
24. Miyoshi, K.; and Buckley, D. H.: Anisotropic Friction and Wear of Single-Crystal Manganese-Zinc Ferrite in Contact with Itself. NASA TP-1339, 1978.
25. Wagner, C. D.; et al.: Handbook of X-ray Photoelectron Spectroscopy. Perkin-Elmer, Physical Electronics Division, 1978.
26. Allen, G. C.; Tucker, P. M.; and Wild, R. K.: Surface Oxidation of Nickel Metal as Studied by X-Ray Photoelectron Spectroscopy. Oxid. Met., vol. 13, no. 3, 1979, pp. 223–236.
27. Pauling, L.: A Resonating-Valence-Bond Theory of Metals and Intermetallic Compounds. Proc. Roy. Soc. (London), ser. A, vol. 196, no. 1046, Apr. 1949, pp. 343–362.
28. Buckley, D. H.: The Metal-to-Metal Interface and Its Effect on Adhesion and Friction. J. Colloid Interface Sci., vol. 58, no. 1, Jan. 1977, pp. 36–53.
29. Miyoshi, K.; and Buckley, D. H.: Adhesion and Friction of Single-Crystal Diamond in Contact with Transition Metals. Appl. Surf. Sci., vol. 6, 1980, pp. 161–172.
30. Buckley, D. H.: Friction and Transfer Behavior of Pyrolytic Boron Nitride in Contact with Various Metals. ASLE Trans., vol. 21, no. 2, Apr. 1978, pp. 118–124.

31. Miyoshi, K.: and Buckley, D. H.: Friction and Wear Behavior of Single-Crystal Silicon Carbide in Sliding Contact with Various Metals. ASLE Trans., vol. 22, no. 3, July 1979, pp. 245–256.
32. Pepper, S. V.: Shear Strength of Metal-Sapphire Contacts. J. Appl. Phys., vol. 47, no. 3, Mar. 1976, pp. 801–808.
33. Kurkjian, C. R.; and Kingery, W. D.: Surface Tension at Elevated Temperatures. III. Effect of Cr, In, Sn, and Ti on Liquid Nickel Surface Tension and Interfacial Energy with Al_2O_3. J. Phys. Chem., vol. 60, 1956, pp. 961–963.
34. McDonald, J. E.; and Eberhart, J. G.: Adhesion in Aluminum Oxide–Metal Systems. AIME Trans., vol. 233, 1965, pp. 512–517.
35. Smithells, Colin J.: Metals Reference Book. Vol. 1, Plenum Press, 1967.
36. Glassner, A.: The Thermochemical Properties of the Oxides, Fluorides, and Chlorides to 2500 K. ANL-5750, Argonne National Laboratory, 1957.

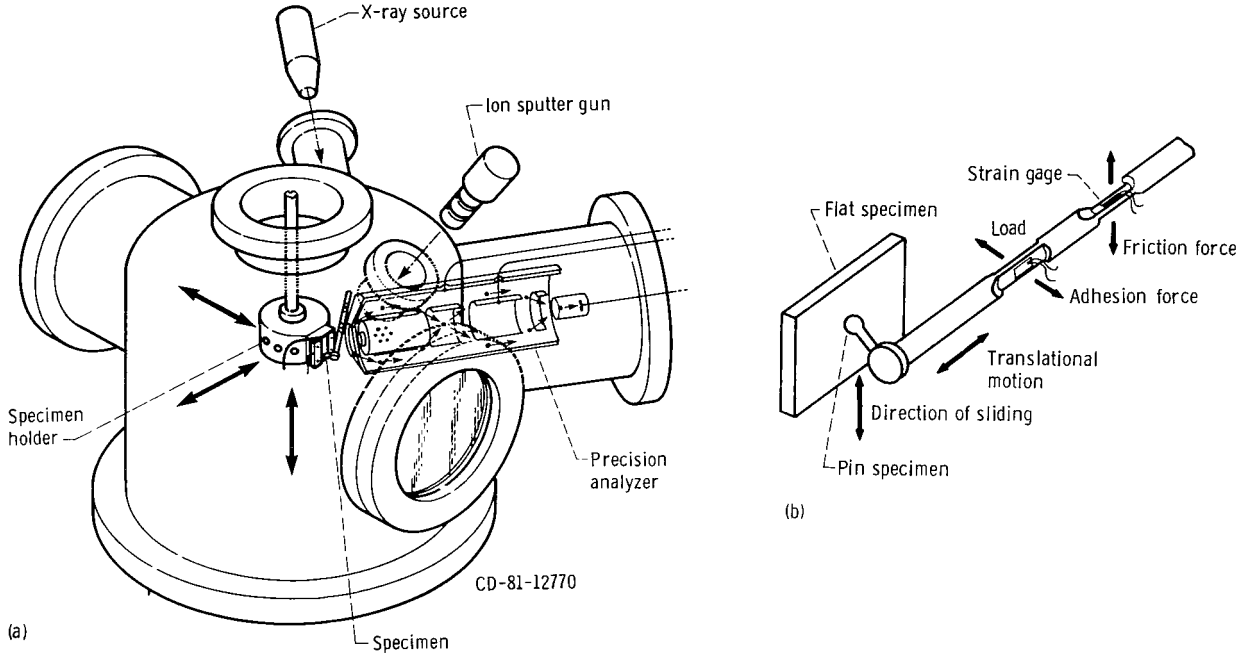

CD-81-12770

(a) Spectrometer.
(b) Specimen holder.

Figure 1. - Schematic representation of X-ray photoelectron spectrometer and friction and wear apparatus.

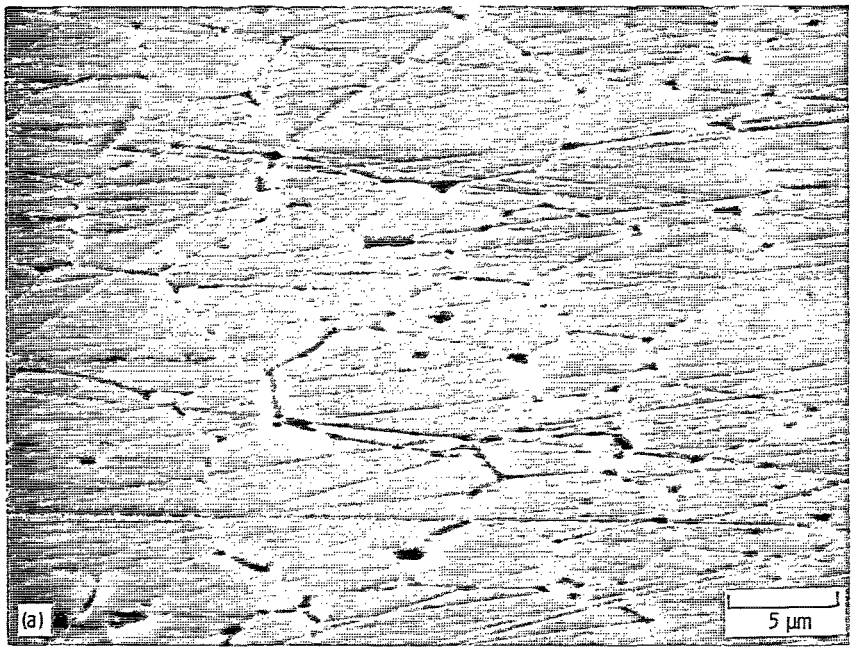

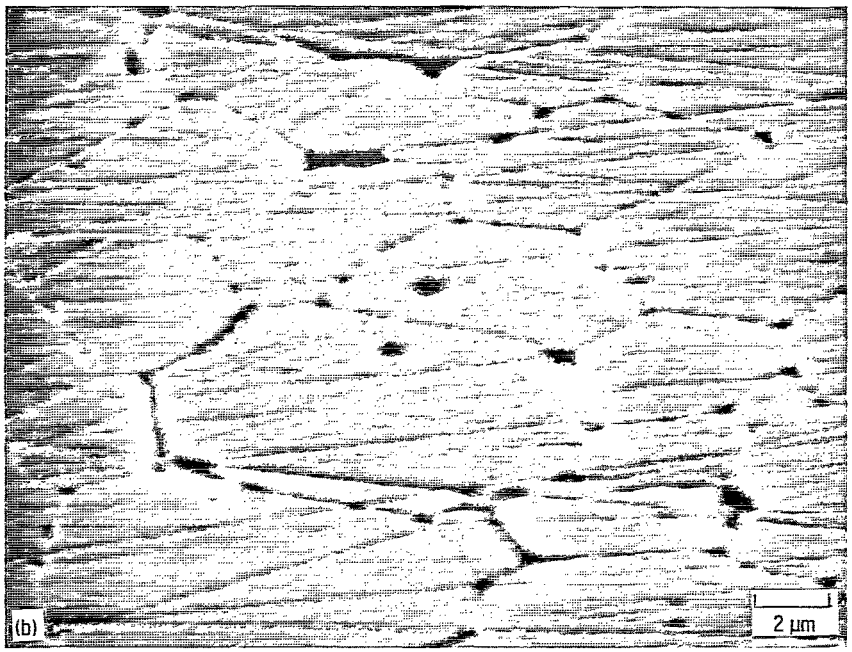

(a) Grain boundary structure.
(b) Grain boundaries, pits, and scratches (high magnification).

Figure 2. - Scanning electron micrographs of chemically etched Ni-Zn ferrite surface.

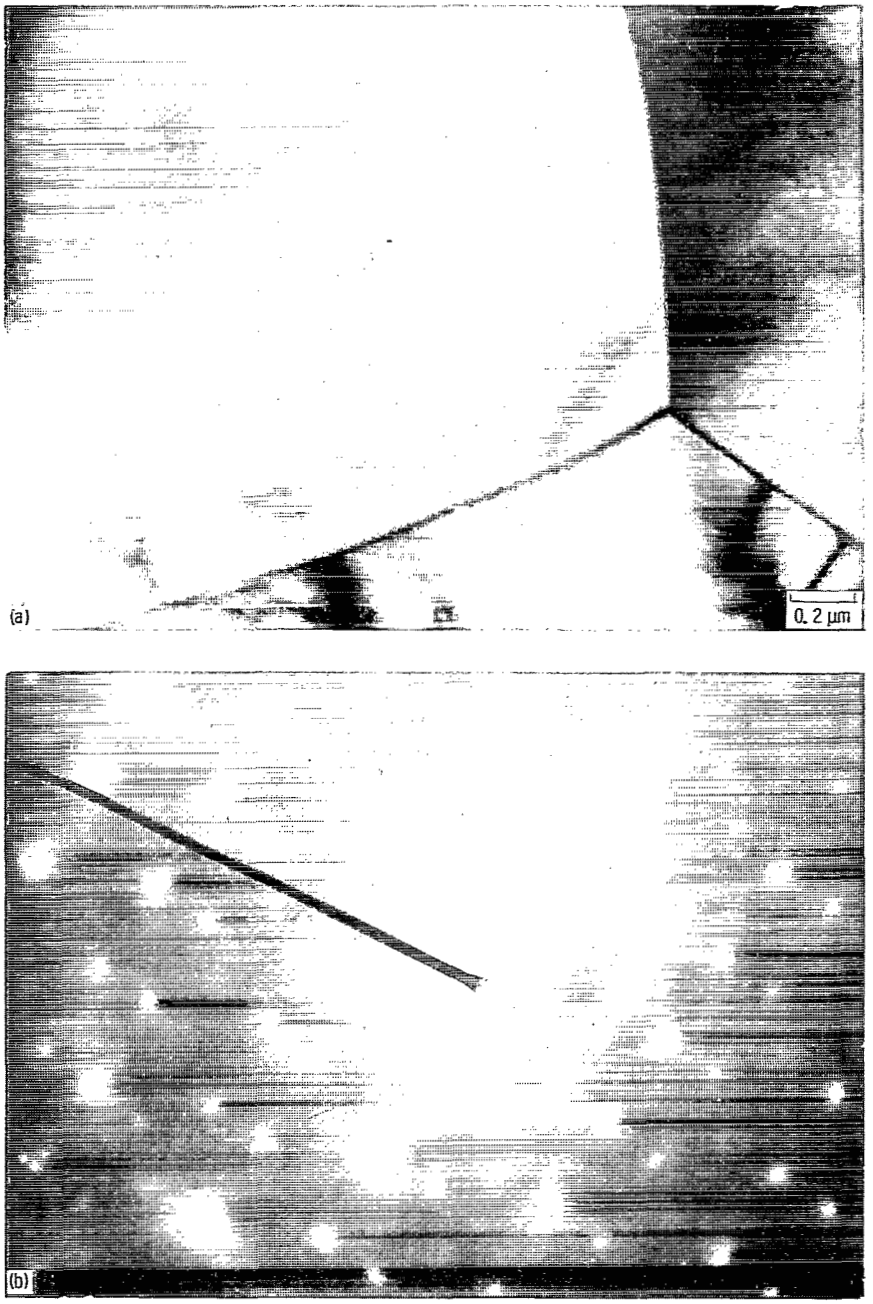

(a) Micrograph.
(b) Diffraction pattern.

Figure 3. – Transmission electron micrograph and diffraction pattern of ion-thinned Ni-Zn ferrite, showing grain boundaries perpendicular to surface.

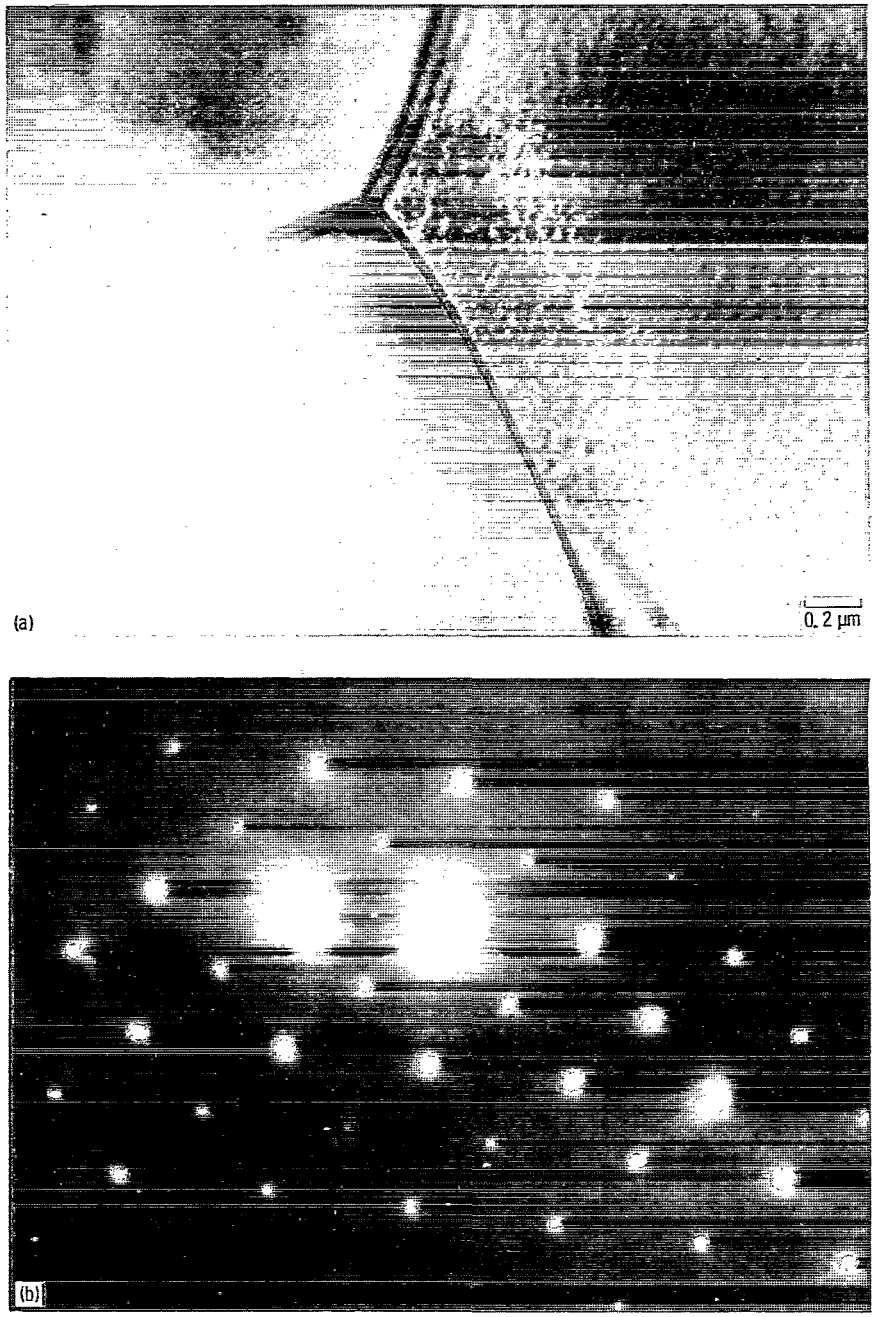

(a) Micrograph.
(b) Diffraction pattern.

Figure 4. - Transmission electron micrograph and diffraction pattern of ion-thinned Ni-Zn ferrite, showing grain boundaries not perpendicular to ferrite surface and containing parallel fringes.

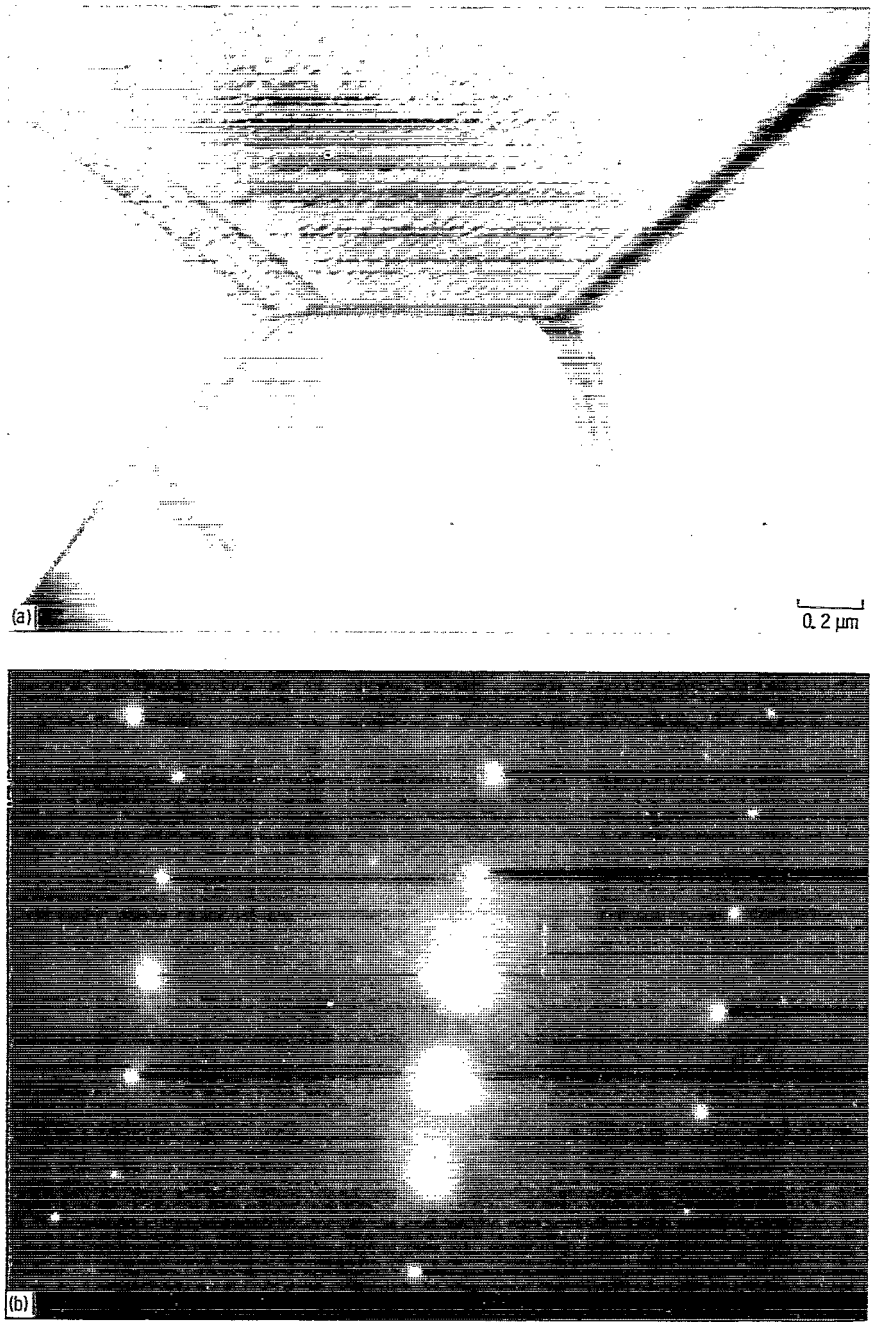

(a) Micrograph.
(b) Diffraction pattern.

Figure 5. - Transmission electron micrograph and diffraction pattern of ion-thinned Ni-Zn ferrite, showing different etch patterns.

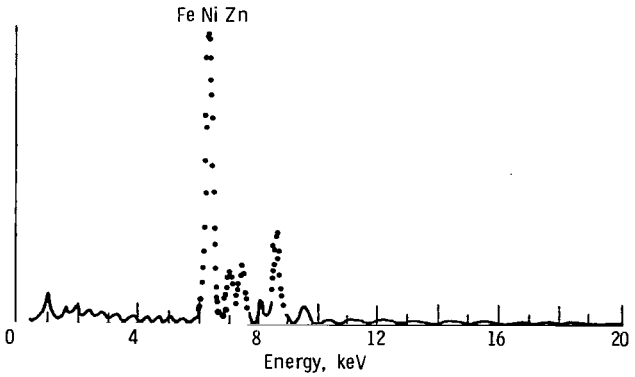

Figure 6. - Energy-dispersive X-ray profile of Ni-Zn ferrite.

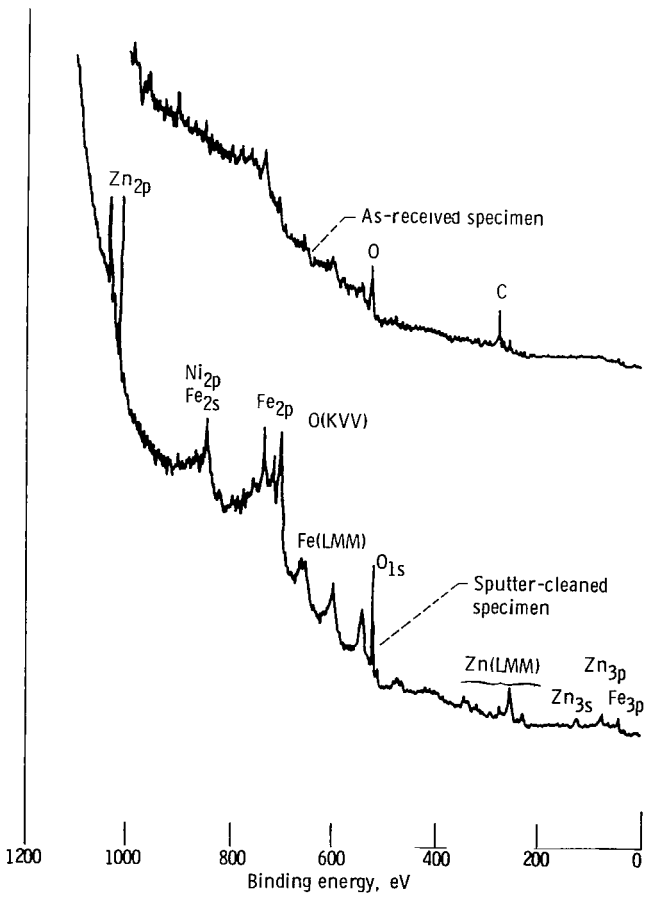

Figure 7. - XPS survey spectral of Ni-Zn ferrite surfaces.

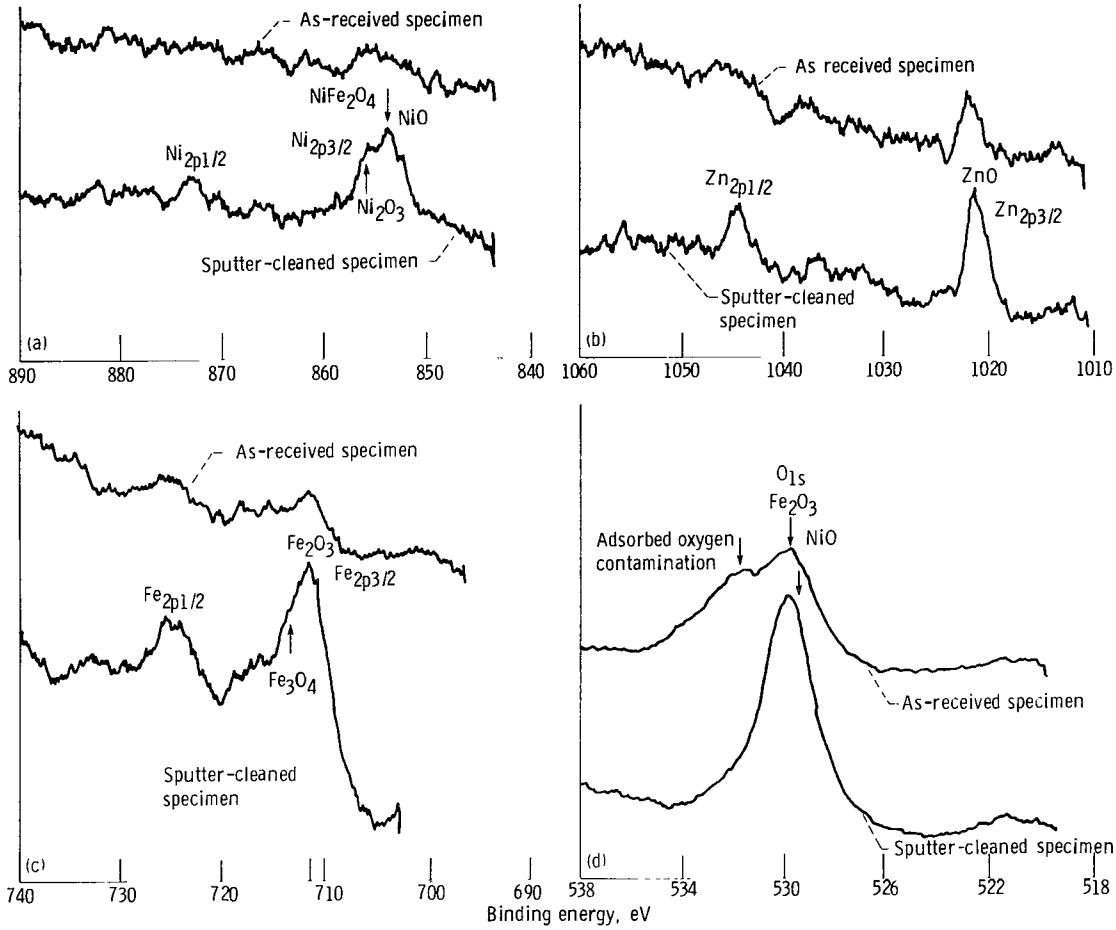

(a) Ni_{2p}. (b) Zn_{2p}. (c) Fe_{2p}. (d) O_{1s}.

Figure 8. - XPS peaks on Ni-Zn ferrite surfaces.

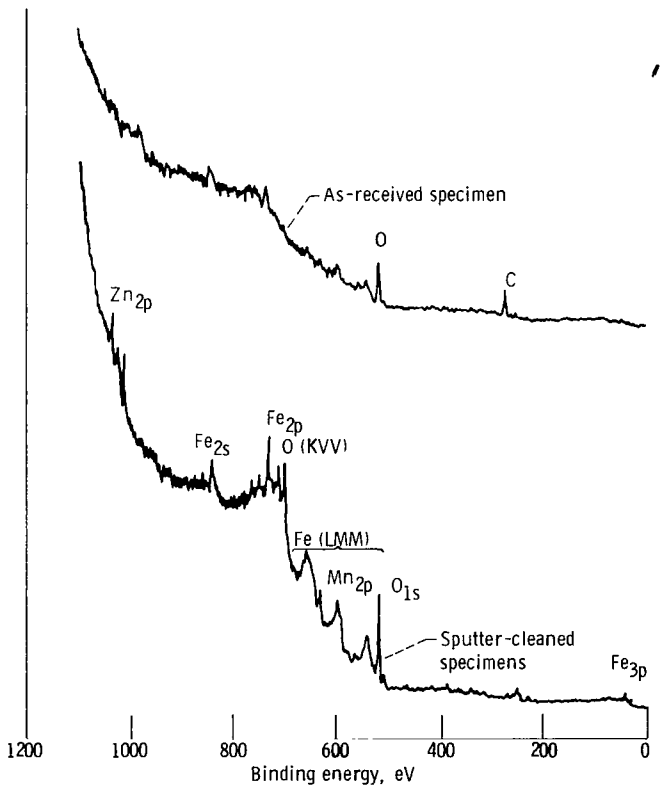

Figure 9. - XPS survey spectra of Mn-Zn ferrite surfaces.

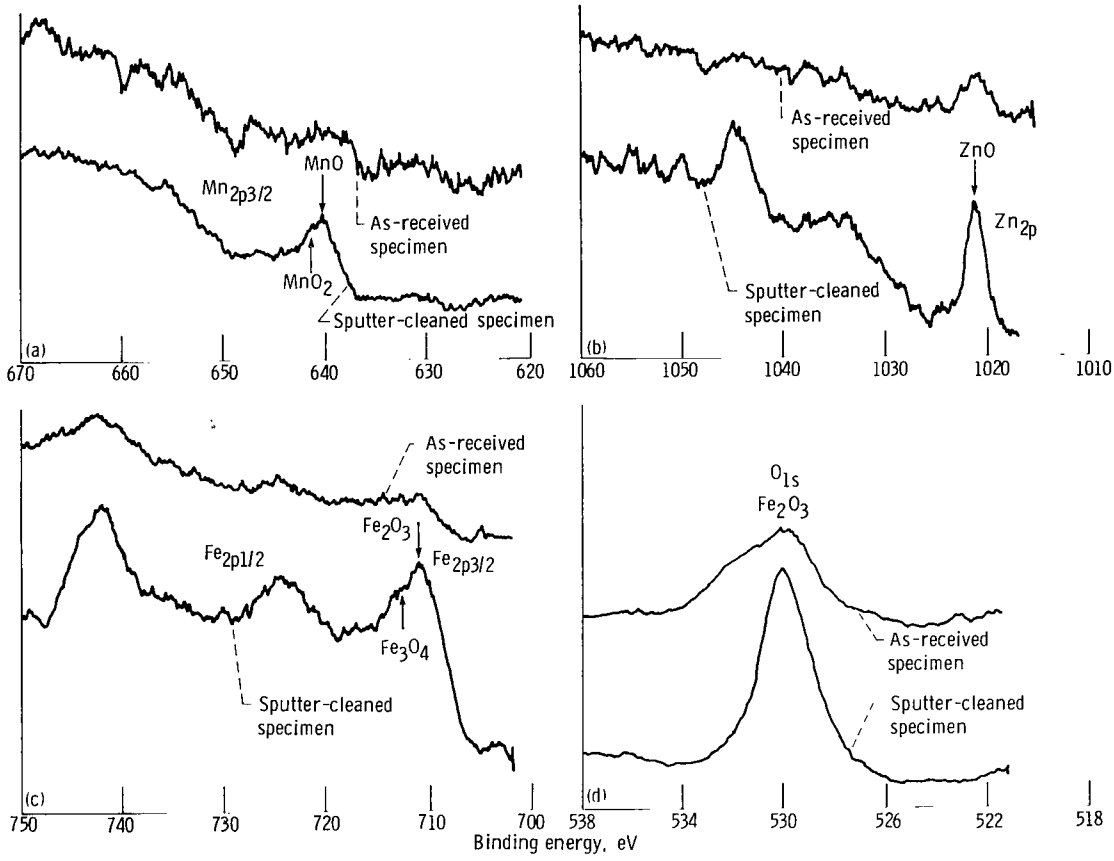

(a) Mn_{2p}. (b) Zn_{2p}. (c) Fe_{2p}. (d) O_{1s}.

Figure 10. - XPS peaks on Mn-Zn ferrite surfaces.

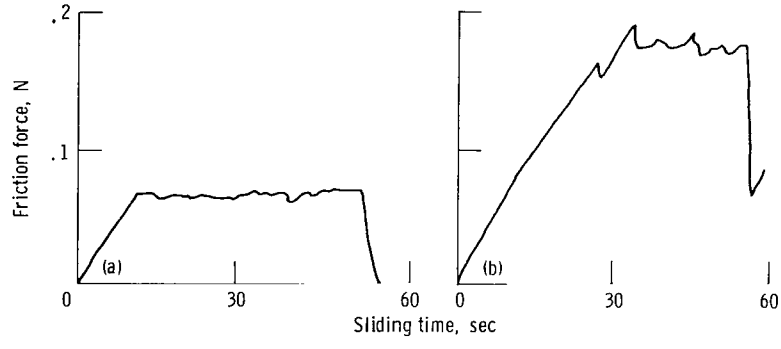

(a) Titanium load, 0.14 N.
(b) Chromium load, 0.1 N.

Figure 11. - Friction traces for metal riders sliding on Ni-Zn ferrite in vacuum (30 nPa). Single-pass sliding; sliding velocity, 3 mm/min; room temperature.

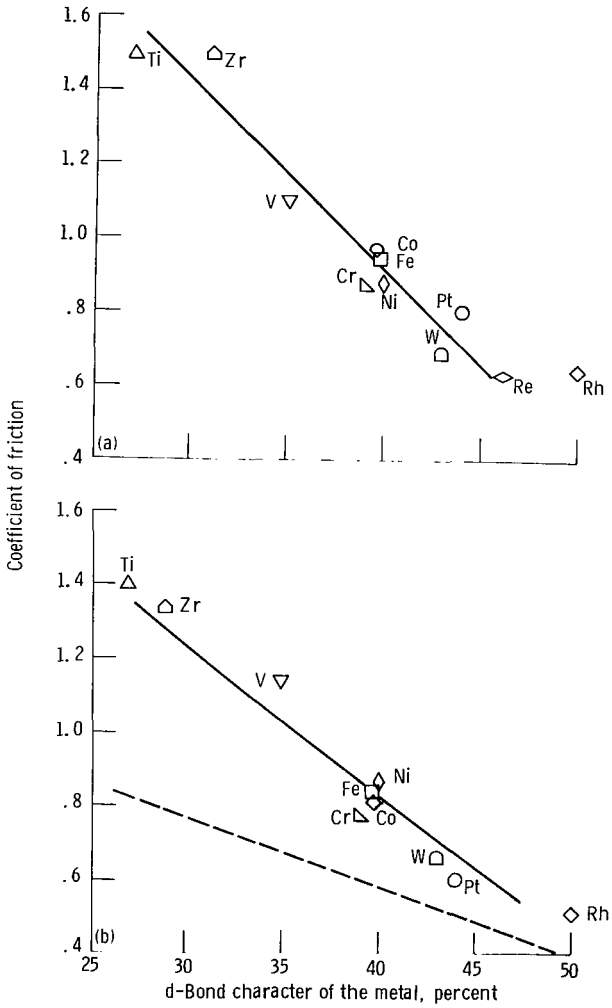

(a) Ni-Zn ferrite.
(b) Mn-Zn ferrite.

Figure 12. - Coefficients of friction as a function of d-bond character of various metals in sliding contact with Ni-Zn and Mn-Zn ferrites in vacuum (30 nPa). Single-pass sliding; sliding velocity, 3 mm/min; load, 0.05 to 0.2 N; room temperature.

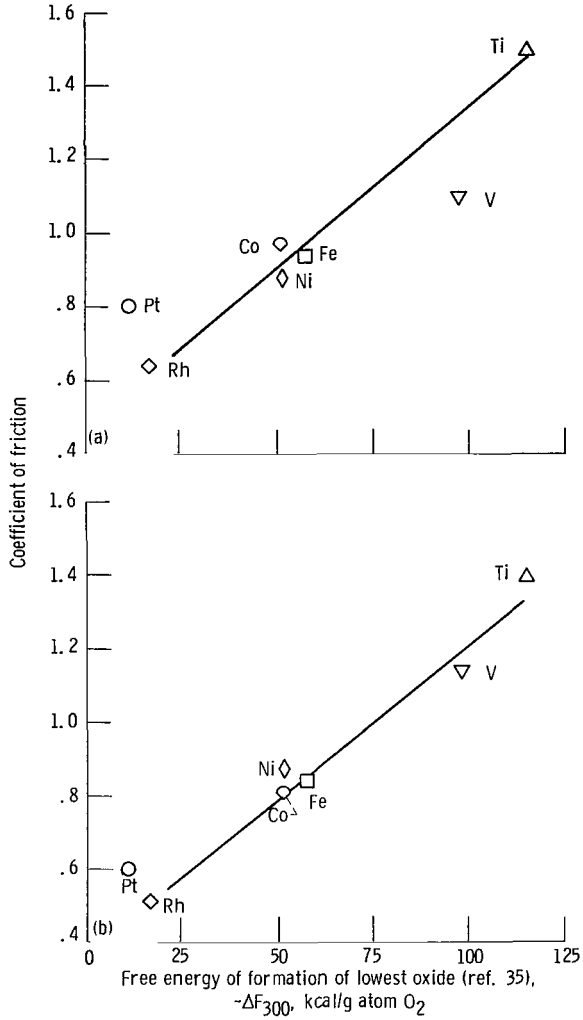

(a) Ni-Zn ferrite.
(b) Mn-Zn ferrite.

Figure 13. - Coefficients of friction as a function of free energy of formation of lowest oxide for various metals in contact with Ni-Zn and Mn-Zn ferrites in vacuum (30 nPa). Single-pass sliding; sliding velocity, 3 mm/min; load, 0.05 to 0.2 N; room temperature.

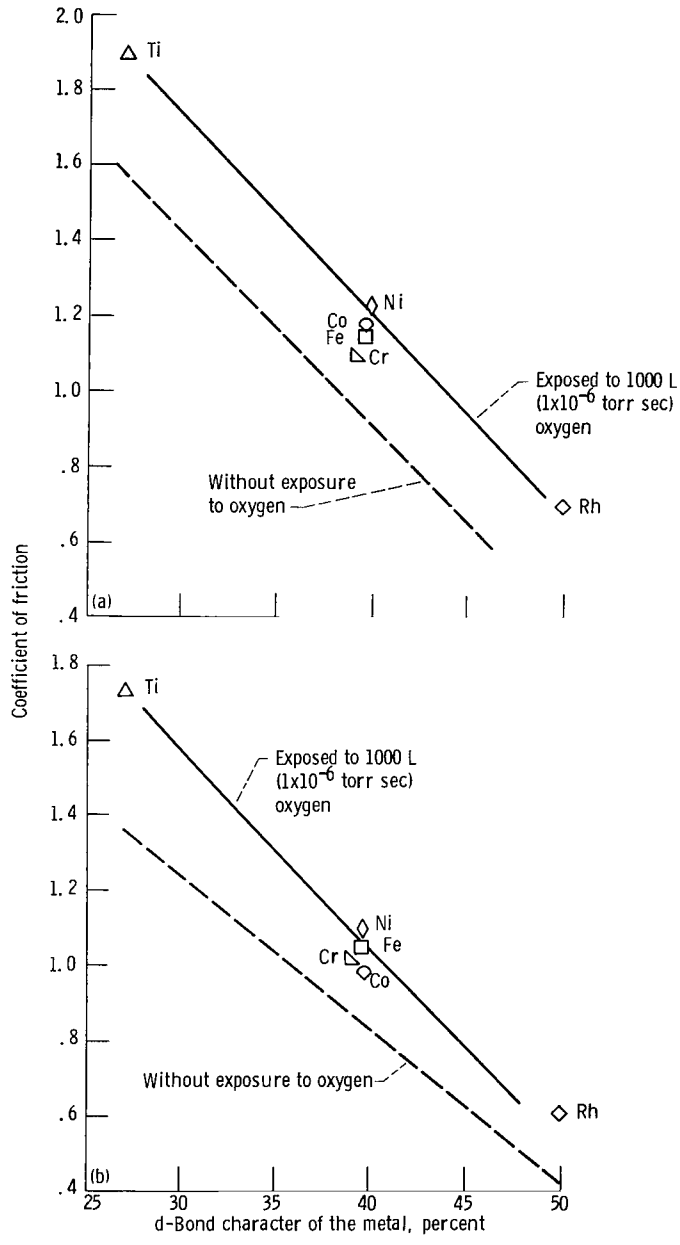

(a) Ni-Zn ferrite.
(b) Mn-Zn ferrite.

Figure 14. - Effect of adsorbed oxygen on friction for various metals in contact with Ni-Zn and Mn-Zn ferrites in vacuum (30 nPa). Exposure, 1000 L (1x10^{-6} torr sec) in oxygen gas; sliding velocity, 3 mm/min; load, 0.05 to 0.2 N; room temperature.

1. Report No. NASA TP-2163	2. Government Accession No.	3. Recipient's Catalog No.
4. Title and Subtitle X-RAY PHOTOELECTRON SPECTROSCOPY AND FRICTION STUDIES OF NICKEL-ZINC AND MANGANESE-ZINC FERRITES IN CONTACT WITH METALS		5. Report Date April 1983 6. Performing Organization Code 506-33-1B
7. Author(s) Kazuhisa Miyoshi and Donald H. Buckley		8. Performing Organization Report No. E-1349 10. Work Unit No.
9. Performing Organization Name and Address National Aeronautics and Space Administration Lewis Research Center Cleveland, Ohio 44135		11. Contract or Grant No. 13. Type of Report and Period Covered Technical Paper
12. Sponsoring Agency Name and Address National Aeronautics and Space Administration Washington, D. C. 20546		14. Sponsoring Agency Code

15. Supplementary Notes

16. Abstract

X-ray photoelectron spectroscopy (XPS) analysis and sliding friction experiments were conducted with hot-pressed, polycrystalline Ni-Zn and Mn-Zn ferrites in sliding contact with various transition metals at room temperature in a vacuum of 30 nPa. The results indicate that the coefficients of friction for Ni-Zn and Mn-Zn ferrites in contact with metals are related to the relative chemical activity in these metals: the more active the metal, the higher is the coefficient of friction. The coefficients of friction for the ferrites correlate with the free energy of formation of the lowest metal oxide. The interfacial bond can be regarded as a chemical bond between the metal atoms and the oxygen anions in the ferrite surfaces. The adsorption of oxygen on clean metal and ferrite surfaces increases the coefficients of friction for the Ni-Zn and Mn-Zn ferrite-metal interfaces.

17. Key Words (Suggested by Author(s))
Ni-Zn ferrite
XPS
Friction

18. Distribution Statement
Unclassified - unlimited
STAR Category 26

19. Security Classif. (of this report)	20. Security Classif. (of this page)	21. No. of Pages	22. Price*
Unclassified	Unclassified	18	A02

* For sale by the National Technical Information Service, Springfield, Virginia 22161 NASA-Langley, 1983